High resolution simulations on the North Aegean Sea seasonal circulation

V. H. Kourafalou, K. Barbopoulos

Annales Geophysicae (2003) 21: 251–265

Annales Geophysicae

High resolution simulations on the North Aegean Sea seasonal circulation

V. H. Kourafalou[1] **and K. Barbopoulos**[2]

[1]National Center for Marine Research, Institute of Oceanography, Athens, Greece
[2]University of Thessaloniki, Division of Environmental Mechanics, Thessaloniki, Greece

Received: 28 June 2001 – Revised: 28 October 2002 – Accepted: 4 November 2002

Abstract. The seasonal characteristics of the circulation in the North Aegean Sea are examined with the aid of a climatological type simulation (three-year run with perpetual year forcing) on a fine resolution grid (2.5 km by 2.5 km). The model is based on the Princeton Ocean Model with a parameterisation of plume dynamics that is employed for the input of waters with hydrographic properties that are different than the properties of basin waters, as the Black Sea Water (BSW) outflow through the Dardanelles Strait and riverine sources. The model is nested with a sequence of coarser regional and basin-wide models that provide for the long-term interaction between the study area and the Eastern Mediterranean at large. The results are employed to discuss the response of the North Aegean to the important circulation forcing mechanisms in the region, namely wind stress, heat and salt fluxes, buoyancy due to rivers and the BSW outflow (which is low in salinity and occasionally low in temperature) and the interaction with the Southern Aegean. The high resolution allows for the detailed representation of the complicated topography that presides in the region. This helps produce a rich eddy field and it allows for variability in the pathways of BSW that has implications in the basin hydrography and circulation.

Key words. Oceanography: general (continental shelf processes; numerical modeling)

1 Introduction

The North Aegean Sea (Fig. 1) occupies the northeastern part of the Eastern Mediterranean, between Greece and Turkey (Asia Minor). It provides a link between the Mediterranean Sea and the Black Sea. The Black Sea Waters (BSW) outflow from the Dardanelles Strait is the most significant quantity of water mass input for the North Aegean. It provides a hydrodynamical connection between the Black Sea and the Mediterranean through the narrow Sea of Marmara. It resembles a massive river, as these waters are characterised by lower salinity than the Aegean waters and they largely exceed the sum of all Aegean river inputs. The BSW outflow also has a temperature signal, so it can be detected in satellite images. The entire Aegean Sea is known as an archipelago, for the hundreds of islands that dot its waters. Being an area that has been marked by the continuous moves of the European, Asian and African tectonic plates, it exhibits remarkable geomorphological variability with a rugged coastline and a plethora of gulfs, bays and peninsulas.

An important feature of the North Aegean bottom topography is the existence of the North Aegean Trough that extends from southwest to northeast (along transect #1, Fig. 1) and includes the deep Sporades, Athos and Limnos basins with depths exceeding 1500 m and separated by sills of about 500 m depth. This provides a natural barrier between the northern shelf areas (marked by the 200 m isobath) and the rest of the domain. Other depressions can be identified in Fig. 1: north and south of the Skyros Island, south of the Sporades Islands and south of the Lesvos Island. A shallow area is found in the vicinity of the Dardanelles (Limnos plateau) and at the northeast (Samothraki plateau), while extensive shelf areas are located west and east of the Chalkidiki peninsula (Thermaikos Gulf and Strimonikos Gulf).

The coastal areas of the North Aegean are highly populated and are the recipients of intense human activities. The knowledge of the circulation is of great interest to the extensive shipping and boating, the commercial and recreational fishing, the tourist industry and to the monitoring and preservation of the coastal ecosystem. We claim that coastal circulation in the area is closely linked to exchanges between the shelf and deep regions. In particular, the path of waters of BSW origin in the upper layers has the potential of affecting coastal areas both directly, by intruding on the shelf, or indirectly, by modifying the overall basin circulation patterns. Another important water mass is the generally saltier and warmer modified LIW (Levantine Intermediate Water), which provides a link with the southern Aegean and influences the hydrographic characteristics of the North-

Correspondence to: V. H. Kourafalou
(villy@rsmas.miami.edu)

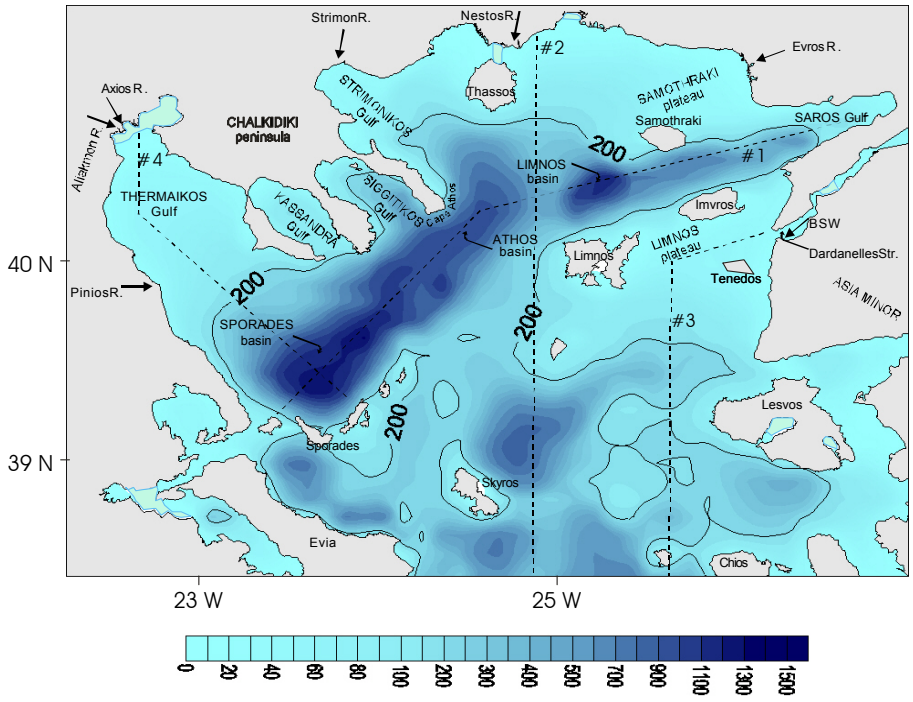

Fig. 1. The North Aegean Sea; arrows mark rivers and BSW (Black Sea Water) inputs; dashed lines mark transects used for the presentation of model results.

ern Aegean intermediate layers.

The objective of this study is to provide the seasonal characteristics of the hydrography and circulation of the North Aegean Sea. In particular, the shelf to deep-sea interactions will be examined and the links between the calculated patterns and the specified inputs will be identified. The pathways of BSW during the different seasons will be discussed, in an effort to better understand the processes that control their transport. As the BSW has been linked to the recent changes in the deep-water characteristics of the Eastern Mediterranean (Zervakis et al., 2000), it is very important to study the initial changes in development for the Dardanelles plume and the consequent route of BSW before exiting toward the South Aegean.

An overview of the oceanography of the Aegean Sea is given in Poulos et al. (1997). They employed climatological values for the hydrological characteristics and the air-sea and land-sea interaction parameters. With the aid of satellite imagery they concluded that the BSW and LIW inputs in the northern Aegean have a pronounced effect on the sea surface temperature and salinity. This was also evident by the studies of Zodiatis (1994) and Zodiatis and Balopoulos (1993) that were based on satellite and in situ hydrographic data. They identified frontal areas linked to water masses of BSW and LIW origin. They found distinctly different patterns for the BSW path between summer and winter, with a pronounced westward transport of BSW across the basin during the summer season, when a path along the northern part of the basin was also identified. Based on recent observations, Zervakis et al. (2000) showed that BSW has the potential to influence dense water formation in the North Aegean.

The North Aegean Sea high-resolution (1/40° by 1/40°) model is coupled with the coarser (1/20° by 1/20°) Aegean and Levantine Eddy Resolving Model (ALERMO, Korres and Lascaratos, 2003), which is also coupled on a Mediterranean OGCM (1/8° by 1/8°, Pinardi et al., 2003). This downscaling approach from basin-wide to limited domains is the key philosophy of the modeling effort within the Mediterranean Forecast System Pilot Project (MFSPP), to ensure that coastal and shelf areas are reasonably linked with the regional seas and with the entire Mediterranean basin.

2 Model description

2.1 Model configuration

A high-resolution hydrodynamic model was applied, in order to simulate the seasonal characteristics of the circulation and density patterns. The model code is based on the three-dimensional, sigma coordinate, free surface, primitive equation Princeton Ocean Model or POM (Blumberg and Mellor, 1983). As this is a widely spread community model, we refrain from a description of the numerics and we refer the reader to the POM home page: http://www.aos.princeton.edu/WWWPUBLIC/htdocs.pom.

The vertical and horizontal eddy viscosity / diffusivity parameters are based on a $2^{1/2}$ order turbulence closure scheme (Mellor and Yamada, 1982) and on the Smagorinski (1963) horizontal advection scheme, respectively.

The present application has adopted the modifications to the basic POM code developed by Kourafalou et al. (1996) and Kourafalou (1999) to include parameterisation of buoyant plumes. Freshwater is discharged in the North Aegean at the mouth of rivers, while waters of Black Sea origin (BSW) that have lower salinity and generally lower temperature (as compared to North Aegean waters) are introduced through the Dardanelles Srait (see Fig. 1). Based on the plume dynamics study of Kourafalou et al. (1996), the modified POM code used here includes: a) the addition of a source term in the continuity equation (external mode) that is equal to the discharge rate divided by the horizontal area of the cell that receives the discharge; b) the specification of salinity for the discharge volume in the advection equation and for the model source nodes. Based on Kourafalou (1999), we also specify different temperature for the BSW inflow. No boundary conditions are needed for the coastal nodes adjacent to the sources, as they are treated as coastal boundaries. Consequently, the values of temperature and salinity in the immediate vicinity of the buoyancy sources are allowed to change, as they are predicted by the model in accordance with the prevailing mixing conditions. This is an advantage over open boundary lateral conditions for river inflows that need specification of temperature and salinity at river mouths.

The model domain extends from 38.6° N to 41.0° N and from 22.5° E to 27.0° E, thus covering both shelf and deep areas in the North Aegean (Fig. 1). The resolution is about 2.5 km by 2.5 km in the horizontal and 16 vertical layers have been implemented unevenly distributed to allow for finer resolution in the upper part of the water column. We have a depth range from 10 m at the coast to about 1500 m at the deep areas; accordingly, a time step of 5 s is specified for the external mode. Based on a Rossby radius of deformation of 6–13 km (Kontoyiannis et al., 2003), the grid spacing is quite adequate for the resolution of eddy features and of flows that are related to the important circulation forcing mechanisms and are modified by the intense topographic features.

2.2 Nesting procedure

As mentioned earlier, we have followed a downscaling approach from the basin-wide, coarse grid Mediterranean OGCM (1/8° by 1/8°), to the regional, intermediate resolution (1/20° by 1/20°) Eastern Mediterranean ALERMO and finally to the high resolution (1/40° by 1/40°) North Aegean Model. The nesting approach is one-way, so that each coarse model influences the solution within the immediate finer one, without any feedback. Attention has been paid to the conservation of volume at the nesting boundaries, to suppress any incompatibilities due to differences in bathymetry. All models use bilinearly interpolated data from the DBDB5 (Digital Bathymetric Data Set 5, compiled by the U.S. Navy), that gives a 1/12° by 1/12° depth resolution. A volume conservation constraint is further applied on the nesting interface. The nesting between the basin-wide and regional models is described in Korres and Lascaratos (2003). Below we give a brief description of ALERMO and the nesting technique with the North Aegean shelf model.

The regional ALERMO model is based on the POM model and has a parameterisation of plume dynamics that is the same as in Kourafalou et al. (1996), i.e. it allows for buoyant sources of different salinity (but not of different temperature, as adopted here for the BSW input). For consistency, the simulations are quite similar, so that the difference in predicted circulation features can be attributed mainly to the higher resolution of the North Aegean Model.

The one-way coupling of the North Aegean Model with ALERMO is along the southern boundary and has the following characteristics:

– Along the nesting interface, 10-day averaged values of sea surface elevation ζ_C, temperature T_C, salinity S_C and velocity (external mode $\overline{U_C}$, $\overline{V_C}$ and internal mode U_C, V_C are provided from the "Coarse" ALERMO model).

– These values are bilinearly interpolated in space (horizontally and also vertically for the three-dimensional parameters) and linearly interpolated in time to provide lateral input $(\zeta'_C, T'_C, S'_C, \overline{U_C}', \overline{V_C}', U'_C, V'_C)$ at each grid point of all model layers and at each time step.

– When V is directed southward (away from the Aegean model computational area), an upstream advection condition is used for T, S. When V is directed northward (toward the model domain), T and S are specified from the interpolated values T'_C, S'_C of the ALERMO model:

$$\frac{\partial T}{\partial t} + V\frac{\partial T}{\partial y} = 0; \quad \frac{\partial S}{\partial t} + V\frac{\partial S}{\partial y} = 0, \quad V < 0$$

$$T = T'_C; \quad S = S'_C, \quad V > 0.$$

– The internal mode velocities are exactly prescribed by the values read at each time step:

$$U = U'_C; \quad V = V'_C.$$

– The external mode (barotropic) velocities normal to the south boundary employ the sea surface elevation ζ and are computed according to the following relation (with ε equal to 1):

$$\overline{V} = \varepsilon\sqrt{\frac{g}{H}}(\zeta - \zeta'_C) + \overline{V_C}',$$

where g is gravitational acceleration and H is depth.

– The tangential barotropic velocities at the south boundary are given by:

$$\overline{U} = \overline{U_C}'.$$

The model boundary was chosen along the narrow passage between the Chios and Evia Islands, which is a natural border between the north and south parts of the Aegean Sea. The areas west of Evia and east of Chios were closed, being too narrow to have an impact on the circulation. The grid line that corresponds to the coupling interface was chosen based on the best match between coarser and finer model bathymetry; small adjustments in the bathymetry of the fine grid model were made, in order to achieve the closest volume match at the coupling interface. A volume conservation constraint was further imposed, as mentioned above.

3 Model simulation

3.1 Initial conditions and forcing fields

The model was initialized with temperature and salinity fields extracted from a climatological run of the regional ALERMO model (Korres and Lascaratos, 2003). The ALERMO model results were available in the form of 10-day averages and were linearly interpolated in time to provide values at each time step and bilinearly interpolated in space, onto the North Aegean Model grid. The initial conditions of salinity and temperature were extracted by the January average of the three 10-day outputs of the ALERMO model. This method was found to be superior to initialization based on the MODB and MEDATLAS databases, which were tested first. The reason is that these bases of oceanographic data lack details on the North Aegean, due to the lack of long-term observations there. Recent in situ data could be inserted, but they are still sporadic in time and space and are not quite suitable for the climatological type of simulation that we attempt here. On the other hand, we want to achieve the best agreement with the regional model, as a test for a successful coupling.

Particular care has been given to the representation of riverine and Black Sea inputs. The development of buoyancy driven circulation in the model is controlled by the amount of discharge, the properties of discharge and the interaction with wind stress and topography. For the rivers, the properties of the run-off were salinity set to zero and a temperature the same as that of the ambient waters. The run-off rates are shown in Table 1 and they are based on climatological annual means (Therianos, 1974); for the Axios, Aliakmonas and Pinios Rivers the values are modified according to measurements obtained during the METRO-MED Project (Dynamics of Matter Transfer and Biogeochemical Cycles: their modeling in Coastal Systems of the Mediterranean Sea), as shown in Kourafalou et al. (2003). For the Dardanelles outflow, we used monthly values of discharge with varying temperature and salinity (Table 2). The discharge rate was calculated based on steady-state water budget calculations (Ünlüata et al., 1990). The temperature and salinity of the outflow are based on data by Besiktepe et al. (1993). A small channel was employed as a crude parameterisation of the Dardanelles, in order to evenly distribute the inflow over several grid boxes, in order to avoid shocking the system.

The atmospheric forcing was based on ECMWF (European Center for Medium Weather Forecast) Re-analysis data for fluxes and wind field. A 15-year data set (1979–1993) was compiled by Korres and Lascaratos (2003) and a perpetual year of atmospheric data was produced, in monthly values. An example is given in Table 3 for a grid point at the Limnos basin. The spatial variability of the wind field is smooth, maintaining a year-round pattern of flow from the northeast with values decreasing from east to west. As seen in Table 3, wind stress reaches a maximum in February, with a secondary maximum in October, presumably associated with the etesian winds.[1]

Table 3 also provides an example of the calculated main heat and salt flux components. These are: the downward solar radiation that is based on the Reed (1977) formula; the net upward flux that includes the longwave radiation (formula by Bignami et al., 1995) and the latent and sensible heat flux calculated by bulk aerodynamic formulae, according to the Kondo scheme for the turbulent exchange coefficients (Kondo, 1975). The net salt flux is due to evaporation minus precipitation multiplied by the salinity at sea surface. The precipitation is based on Jaeger's (1976) monthly precipitation data, while evaporation was calculated from the latent heat flux. A detailed description of the calculation of the surface fluxes is given in Korres and Lascaratos (2003).

Several sensitivity tests were made on the model's response to the parameterisation of air-sea interaction. These tests were a follow-up of the ALERMO simulations, which were based on the Mediterranean OGCM calculations. Thus, the heat and salt flux calculations were similar for the basin-wide, the regional and the shelf models. Here we present simulations based on the parameterisation that we found most satisfactory, namely corrected heat fluxes directly based on the ALERMO results, which were also adjusted based on the fluxes calculated by the OGCM. A flux correction term was added on all simulations, relaxing the computed temperatures to "climatological" values. In the sequence of nested simulations, these values were taken from a) the MODB-MED4 SST seasonal climatology (Brasseur et al., 1996) for the OGCM; b) the OGCM 8th year simulation for the ALERMO; c) the ALERMO 2nd year simulation for the North Aegean Model.

3.2 Seasonal results

We performed a 3-year simulation with the perpetual year forcing described in the previous section. The North Aegean Model results for the second and third years were quite similar, which indicates that the length of the simulation is adequate for the discussion of seasonal patterns.

We present here seasonally averaged results from the third year of the simulation. The definition of the seasons

[1] From the greek word "etesios", meaning "annual"; refers to cool and strong winds from the north-northeast that dominate the Aegean over several day periods, generally in summer to autumn.

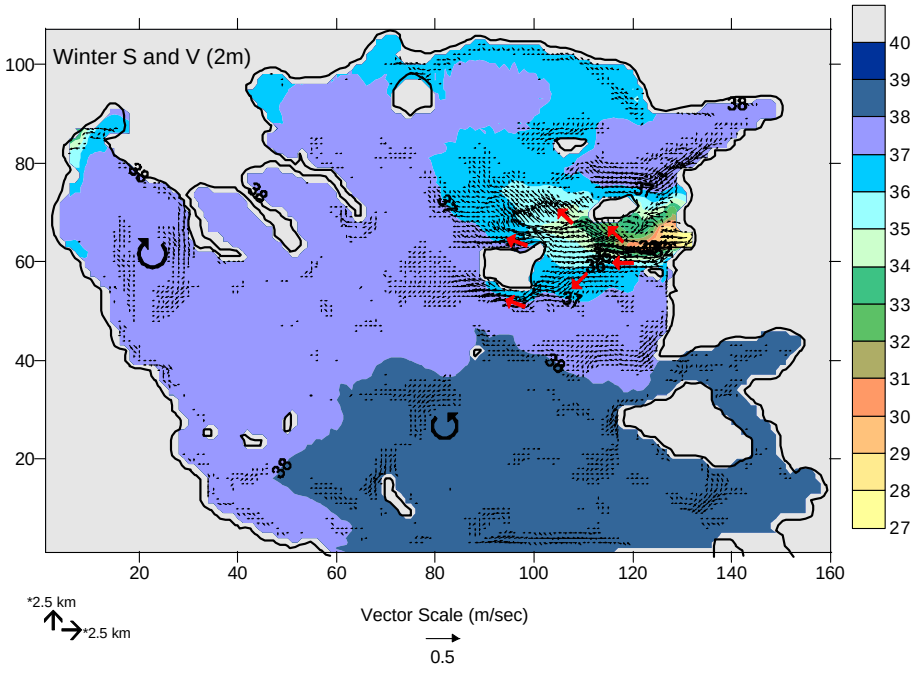

Fig. 2. Model computed salinity and current velocity at 2 m for the winter season (minimum velocity: 5 cm/s); red arrows denote dominant pathways for waters of BSW origin; curved black arrows mark prominent eddies.

is as follows: winter (December-January-February); spring (March-April-May); summer (June-July-August); autumn (September-October-November). We first present horizontal plots of temperature, salinity and velocity, where we identify the dominant gradients and circulation features. We have marked the dominant pathways for the waters associated with the outflow at Dardanelles (BSW waters); the important eddies are also pointed out. Then, we examine vertical cross sections along the major North Aegean basins, in order to discuss the vertical structures and the differences among the water masses within the deep sub-basins.

3.2.1 Winter season

Figure 2 shows the near-surface salinity and current velocity distribution during the winter season. The plume associated with the BSW outflow is evident, occupying the area with lowest salinities. There is a marked difference in salinity between the southern and northern parts of the domain, which is maintained throughout the year: higher salinity in the south, associated with the characteristics of South Aegean waters and lighter salinity in the north, associated with the effect of the BSW. However, this difference is moderate in winter (with respect to subsequent seasons, as we will discuss below), as the BSW waters are mostly concentrated near the Dardanelles and the Limnos plateau. The temperature field (not shown) exhibits generally cool waters (less than about 14°C), with slightly warmer waters intruding from the south Aegean. There is evidence of stronger cooling on the shelf areas, especially on the broad Thermaikos plateau. The velocity field is most prominent near the BSW outflow, where buoyancy and wind stress combine to advect the brackish waters. There are two dominant branches, north and south of the Limnos Island, the northward one being more effective in lowering the salinity of a large portion of the northeastern Aegean and of part of the northern shelf areas. An anticyclonic eddy is formed on the Thermaikos plateau, occupying cooler waters that were formed on the shelf there. A cyclonic eddy is found on the deeper part of the northern Skyros basin, associated with the frontal area between colder N. Aegean waters and warmer waters intruding from the southern Aegean. Two weak cyclonic eddies are not marked: at the Sporades basin and at the depression south of Lesvos island. Coastal flows are formed everywhere, especially near river sources.

Analysis of results in deeper layers (not shown) reveals that the intermediate waters are influenced by the interaction of basin waters with the warmer and saltier waters of LIW origin. At 100 m the eddy field is quite energetic, especially along the N. Aegean trough. A series of cyclonic eddies is present along the Limnos basin, with a strong anticyclone in the Athos basin and two strong cyclones in the Sporades basin (deep and shallow parts); the latter are connected to the weak signal at 2 m, mentioned above. The near-surface cyclone that was seen north of Skyros Island in Fig. 2 is strengthened, while a strong anticyclone is also present south of Lesvos Island (which has a moderate signal on the near-surface field in Fig. 2). The latter features are still evident, but weakened, at 300 m. At this level the Athos anticyclone is a strong feature, with a cyclonic eddy pinching off toward the Athos Gulf. Both eddies in the Sporades basin have turned anticyclonically.

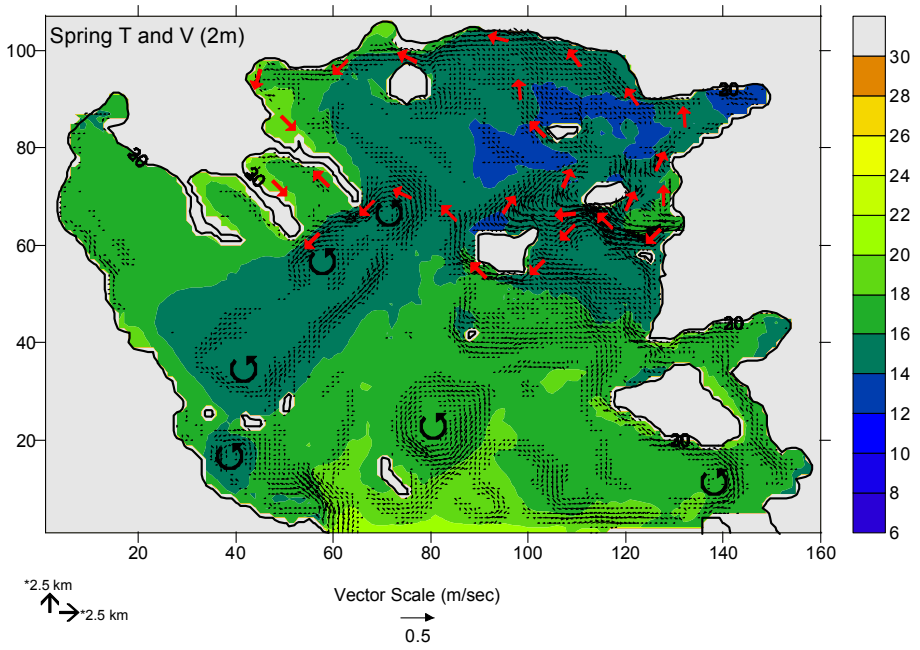

Fig. 3. Model computed temperature and current velocity at 2 m for the spring season (minimum velocity: 5 cm/s); red arrows denote dominant pathways for waters of BSW origin; curved black arrows mark prominent eddies.

3.2.2 Spring season

Figure 3 shows the near-surface temperature and velocity fields during spring. Temperatures are higher than in winter, with the highest temperatures in the south (due to South Aegean influence) and at the shallow shelf areas (due to a faster response to the imposed heat flux). Coolest areas are found along the N. Aegean trough and especially at the Limnos basin, where they remain at winter levels. A small area around the Dardanelles is slightly cooler than ambient waters, due to the low temperature of the Dardanelles inflow in the spring season (Table 3). Cool waters are also found along portions of the Asia Minor coast, indicative of upwelling. Based on the salinity field (not shown), we have marked the dominant pathways of BSW. Several paths can be seen, starting with a spreading of the brackish waters at the north, west and south. The northward branch freshens the shelf areas of the southeastern and northern Aegean, strengthening buoyancy-driven flows due to local rivers. The southward branch turns anticyclonically and joins the westward branch, which then splits twofold around the Limnos Island: toward the west and then north, following a more direct pathway toward the northern shelf areas; and toward the south and then northwestward, bringing low-salinity waters to the Athos basin. Several cyclonic eddies are marked on Fig. 3, some in similar locations as in the winter season. We note that the Skyros eddy remains cyclonic, while the Sporades and Lesvos eddies rotate anticyclonically, i.e. opposite than in the winter season.

A remarkable intrusion of waters of LIW origin takes place in the intermediate levels. At 100 m (Fig. 4) the flow of these waters is marked, following a cyclonic meandering pattern from the south toward north and then southwestward, thus influencing the properties of the intermediate layers in the N. Aegean. A double cyclonic-anticyclonic eddy system is found south of Lesvos, while the Sporades basin eddy is anticyclonic. This is still evident at 300 m depth, where the Lesvos eddy is also anticyclonic.

3.2.3 Summer season

The near-surface summer salinity and current velocity fields are shown in Fig. 5. The plume associated with BSW outflow is strongest, depicting an intense anticyclonic bulge in the vicinity of the Dardanelles and a secondary anticyclonic bulge immediately south. The BSW waters exhibit a wider range of pathways as compared to the previous seasons. A strong tendency for northeastward transport can be seen, that is responsible for the evident freshening of a large portion of the north part of the domain. The northwestward flow is first channeled between the Imvros Island and Asia Minor (with a smaller branch south and around Imvros), then it branches around the Samothraki Island. An anticyclone forms on the Samothraki plateau. The north branch fills the northern shelf area. The south branch flows along the shelfbreak, partially into the Strimonikos Gulf and mostly toward the south, entering the Gulfs of Athos and Kassandra, and then eastward and southward, along the western coast, exiting toward the south Aegean. Another main pathway is triggered by the part of the outflow that is initially channeled southward, between the Tenedos Island and Asia Minor. Waters along this pathway move westward in a more direct way, freshening the central part of the domain and joining the branch around the Sporades Island, finally exiting toward south. The most

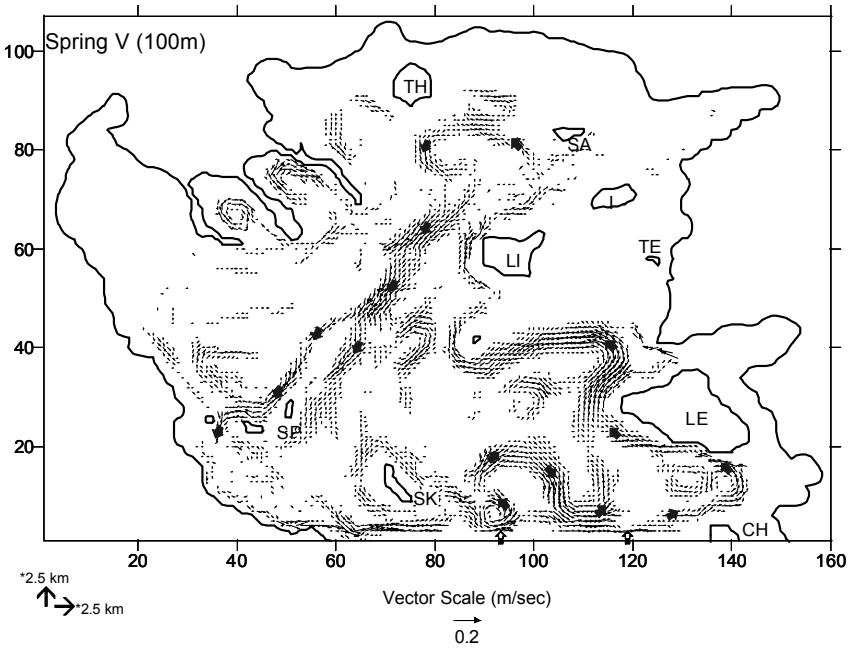

Fig. 4. Model computed current velocity at 100 m for the spring season (minimum velocity: 3 cm/s); black arrows denote dominant pathways for waters of LIW origin. Islands are marked as SA: Samothraki; TH: Thassos; I: Imvros; LI: Limnos; SP: Sporades; TE: Tenedos; LE: Lesvos; SK: Skyros; CH: Chios.

prominent eddy features are the Athos and Sporades anticyclones. The intermediate layers exhibit strong eddy activity. An example is shown in Fig. 6 for flow at 300 m. The Sporades eddy and Lesvos eddies are anticyclonic; a pair of cyclones is seen south of the Thassos Island and a pair of cyclone/anticyclone is found south of Chalkidiki; the Skyros eddy is cyclonic.

The near-surface temperature field (not shown) is dominated by east to west gradients with cooler temperatures at the east, especially along the entire Asia Minor coast (minimum temperatures there are about 17°C). Examination of vertical structures there clearly indicates upwelling; this is presumably the cause of the strong east-west temperature gradient. The shallow areas along the north part of the domain are warmest, with certain temperatures exceeding 30°C. The Dardanelles outflow has similar temperature with that of ambient waters. Gradients related to LIW inflow from the southeast are more confined with respect to the spring season.

3.2.4 Autumn season

Figure 7 shows the near-surface salinity and current fields for the autumn season. The strength of the plume near the Dardanelles is diminished with respect to the summer season, so that the anticyclone associated with the plume is confined between Asia Minor and the Tenedos Island. The northward pathway for BSW is also diminished, but is strong enough to bring low-salinity waters in the Strimonikos Gulf. The dominant pathway is westward, starting with flow around the Limnos Island. It then follows a similar path as in the summer season, exiting southward along the western part of the domain. A secondary branch brings low salinity waters in the Thermaikos Gulf, entering from the west and exiting from the east, marking a strong anticyclone and affecting the salinity of a large portion of the Gulf. Anticyclonic circulation is also marked south of Athos and on the northeastern Aegean shelf. The Samothraki anticyclone is strengthened, as compared to the summer season and it causes southward advection of the low salinity waters that are associated with the Evros River plume. The Sporades eddy is cyclonic and a smaller cyclone is located south of the Sporades Islands, partially blocking the southward exit of BSW.

Temperatures (not shown) are cooler than in summer, with highest values in the shelf areas, where they reach 24°C. The gradient is now mostly north to south, but an east to west gradient is maintained south of the Dardanelles, with cooler temperatures along the Asia Minor coast. The BSW outflow is cooler than the ambient waters, with a well-marked westward tongue of cool waters, along the pathway marked in Fig. 7. The anticyclone on the northeastern shelf seems to be related to a temperature gradient between warmer shelf waters and cooler waters intruding from east. The intrusion of waters of LIW at intermediate levels is more evident than in summer, but less pronounced than in spring, influencing mainly the southeast part of the domain. At these levels, there is a tendency for flows opposite to the near-surface flows associated with the dominant BSW pathway described above.

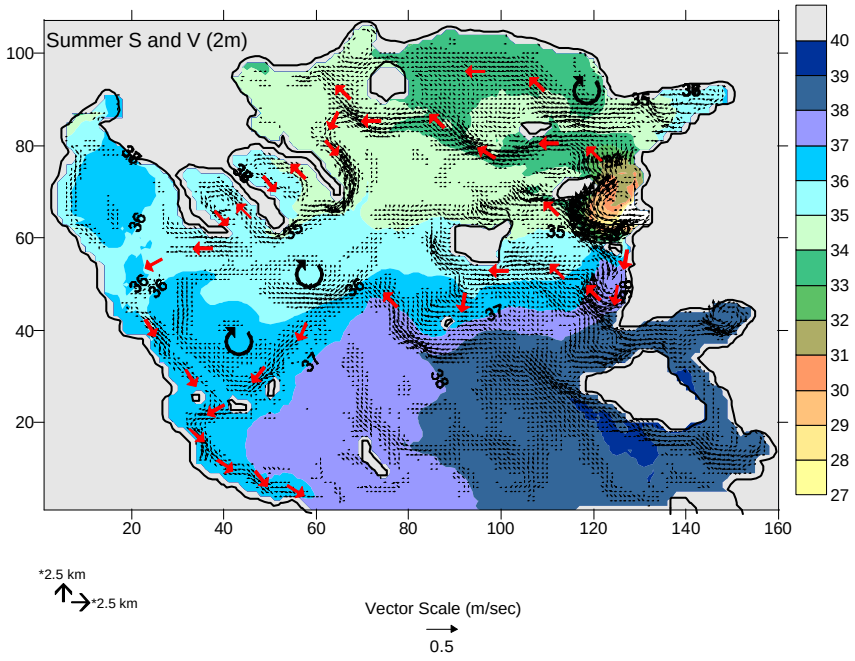

Fig. 5. Model computed salinity and current velocity at 2 m for the summer season (minimum velocity: 5 cm/s); red arrows denote dominant pathways for waters of BSW origin; curved black arrows mark prominent eddies.

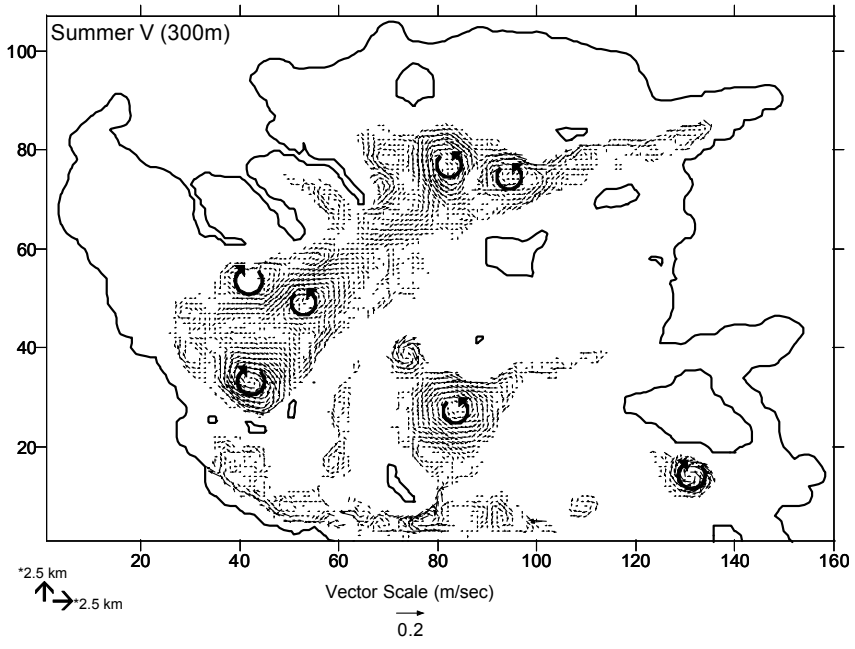

Fig. 6. Model computed current velocity at 300m for the spring season (minimum velocity: 1 cm/s); curved black arrows mark prominent eddies.

3.2.5 Vertical cross sections

We examine vertical structures along the transects marked in Fig. 1. The sections are chosen through the North Aegean trough (transect 1), from north to south in the middle of the domain (transect 2), through the Dardanelles plume and to the south in the eastern part of the domain (transect 3) and along the Thermaikos Gulf and the Sporades Basin (transect 4). The results that are discussed below are plotted with the shallow part of the section at the right side. For clarity, temperature is plotted every 0.5°C and salinity is plotted every 0.3 psu.

Figure 8 shows temperature at transect 1 for the winter and summer seasons. The deep areas correspond to the Lim-

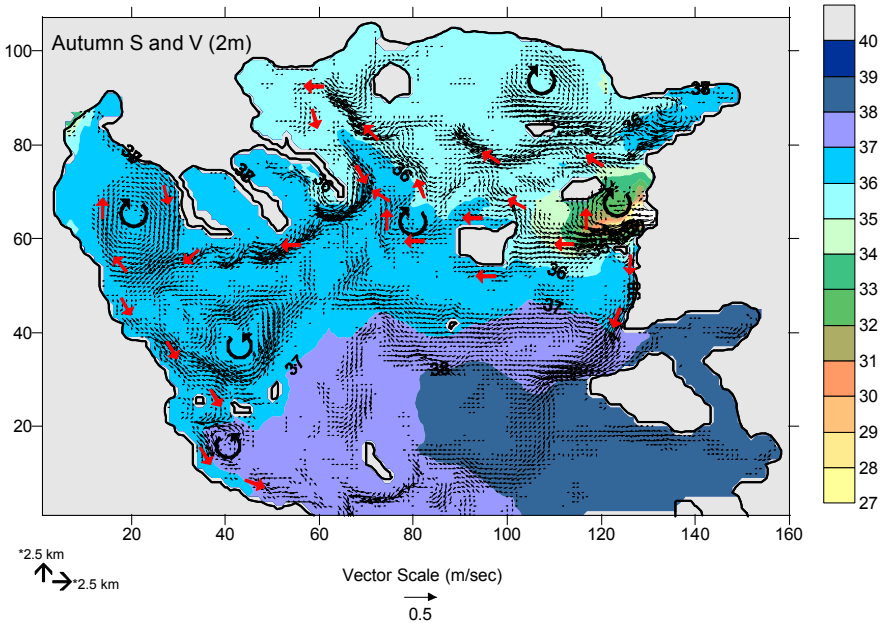

Fig. 7. Model computed salinity and current velocity at 2 m for the autumn season (minimum velocity: 5 cm/s); red arrows denote dominant pathways for waters of BSW origin; curved black arrows mark prominent eddies.

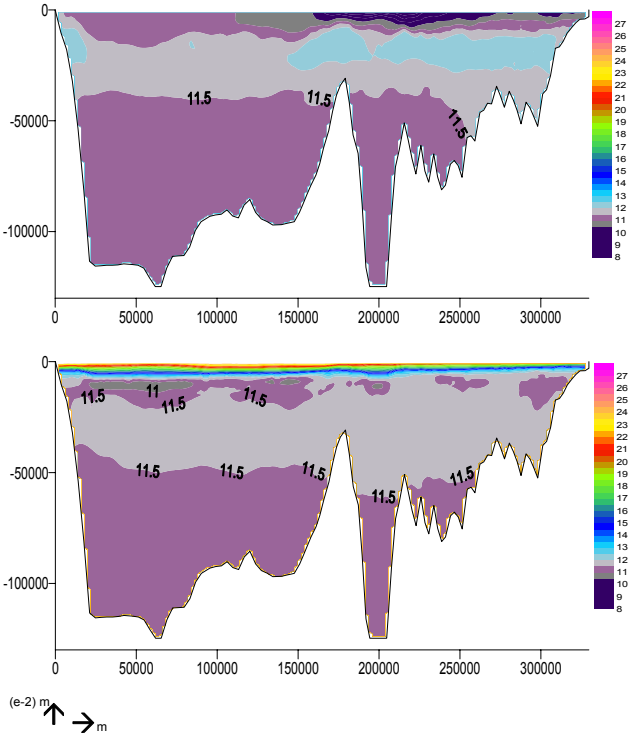

Fig. 8. Temperature cross-section 1 (transect shown on Fig. 1). Winter (upper panel) and Summer (lower panel).

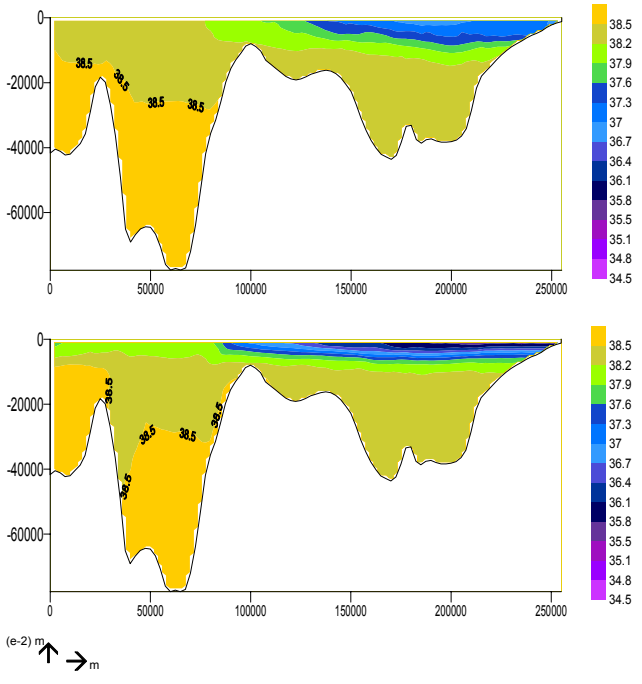

Fig. 9. Salinity cross-section 2 (transect shown on Fig. 1). Spring (upper panel) and Autumn (lower panel).

nos, Athos and Sporades basins (from right to left). In winter, coolest waters are found near surface in the Limnos and Athos basins, where a marked intrusion of a warmer intermediate layer can be seen. The summer section has the highest temperatures near surface at the Sporades basin, with a strong thermocline all along. A cooler intermediate layer exists, where patches of cold waters are trapped. The most pronounced such patch is in the Sporades basin, with a temperature lower than the surface temperature there in winter, but similar to that of the surface layer along the Athos and

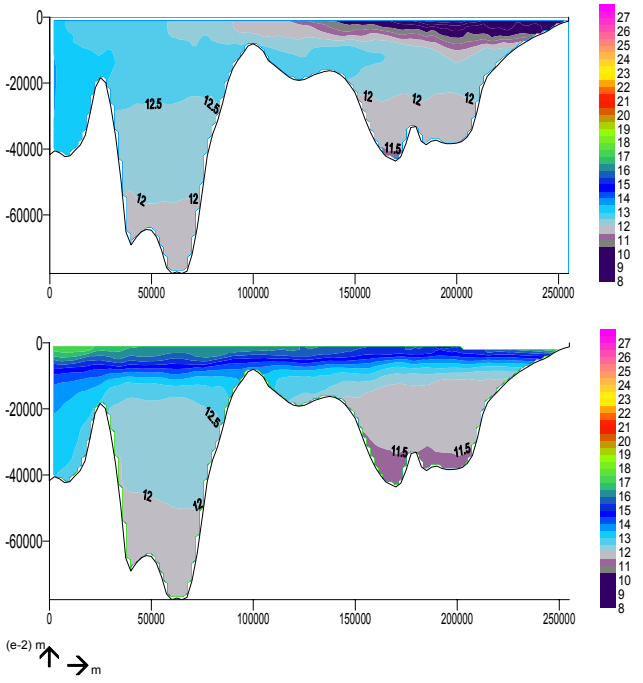

Fig. 10. Temperature cross-section 2 (transect shown on Fig. 1). Winter (upper panel) and Autumn (lower panel).

Limnos basins. Examination of the temperature section in spring reveals that this cold surface layer that is observed in winter is trapped below surface at the onset of stratification and expands eastward. The salinity sections are dominated by a thin layer of low-salinity waters near surface that is pronounced mainly at the Limnos basin and expands eastward in summer and autumn.

Salinity along transect 2 is presented in Fig. 9 for the spring and autumn seasons. The effect of BSW is obvious, covering a larger portion of the basin in autumn. This is a trend that started in spring and continued through the summer and autumn seasons. The southern part of the basin (left part of plots) is also less saline near surface in autumn than in winter, as expected from comparison of Figs. 2 and 7. The winter temperature field (Fig. 10) shows very cold waters near surface at the north shelf area, with a signal near bottom. These waters form cold patches at intermediated levels during spring and summer (not shown) and fill the bottom layer in autumn (Fig. 10).

The results along transect 3 are shown in Figs. 11 (salinity) and 12 (temperature). Vertical stratification associated with the Dardanelles plume is evident in all seasons, as the outflow has different properties than the surrounding waters. The plume has the strongest salinity signal in autumn (Fig. 11) and summer, as these are the seasons that combine a high discharge rate and low salinity for the outflow (Table 1). Winter (Fig. 12) and autumn exhibit the strongest temperature signal, with plume waters clearly cooler than ambient waters. It is evident that strong stratification is connected with the Dardanelles plume, even in the winter and autumn seasons, when

Table 1. Annual discharge rates of North Aegean Rivers

Rivers	Discharge rate (m^3/s)
Evros	100
Nestos	50
Strimonas	100
Axios	130
Aliakmonas	60
Pinios	75

Table 2. Monthly Evolution of the Black Sea Water outflow properties

Time (Months)	Temperature (°C)	Salinity (psu)	Outflow (m^3/sec)
January	10.50	26.27	5700
February	8.75	26.88	7500
March	7.0	27.50	10 000
April	14.25	24.05	12 500
May	17.5	23.53	14 300
June	20.5	23.01	15 000
July	23.5	22.50	14 300
August	21.0	23.13	12 500
September	18.8	23.77	10 000
October	16.4	24.41	7500
November	14.0	25.05	5700
December	12.25	25.66	5000

winds are the strongest (Table 2). The southern part of the section (left part of plots) is not affected by the BSW outflow, but connected with influences from the southern Aegean.

The salinity and temperature fields along transect 4 are presented in Figs. 13 and 14, respectively. The shallow part of the section (Thermaikos Gulf, right part of the plots) is occupied by low-salinity waters year-round, due to local riverine sources. A removal mechanism of these waters toward the south in the middle of the Gulf is indicated in Fig. 13, during winter, when a blob of low salinity waters is found at the surface layer of the Sporades basin. A remarkable intrusion of low-salinity waters is seen in the temperature section for the autumn season, which was attributed to the intrusion of BSW, based on the findings shown in Fig. 7. The temperature vertical profiles show that during summer a thin warm layer extends to the Sporades basin. There is evidence of cool Thermaikos waters descending toward the Sporades basin in spring (not shown), so that they form a cool sub-surface layer that is maintained in summer (Fig. 14). Cooling of the surface layers starts again in autumn (Fig. 14), where there is a marked difference between the Sporades basin and Thermaikos Gulf. This is probably due to the fact that the Gulf waters were very warm during summer and they have not lost enough heat to reach offshore temperatures. The subsurface cool layer that is evident in summer disappears during

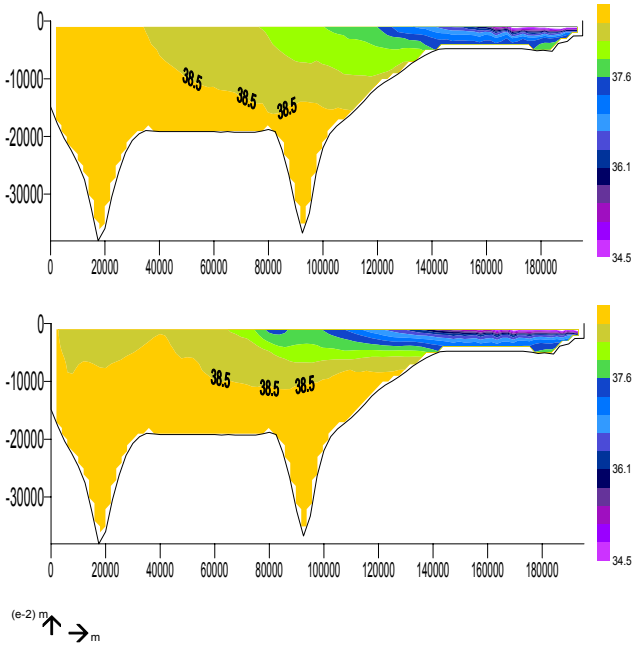

Fig. 11. Salinity cross-section 3 (transect shown on Fig. 1). Winter (upper panel) and Autumn (lower panel).

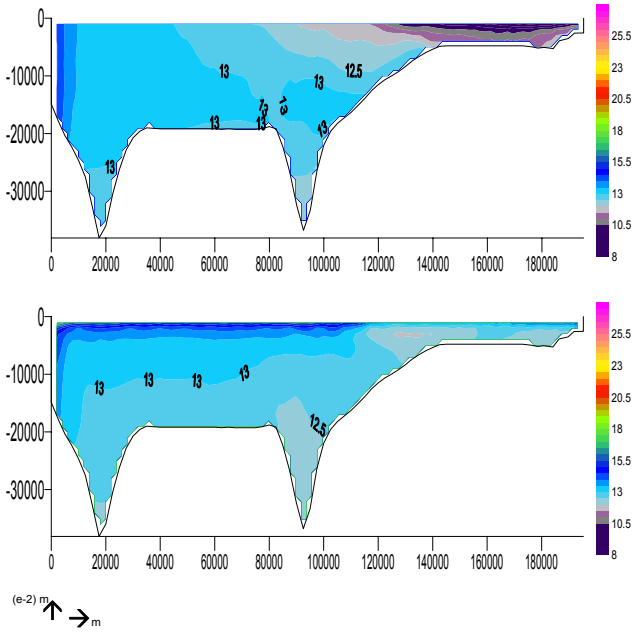

Fig. 12. Temperature cross-section 3 (transect shown on Fig. 1). Winter (upper panel) and Spring (lower panel).

autumn, so that the colder waters occupy both deep and intermediate layers.

4 Discussion and concluding remarks

The model computed horizontal and vertical distributions of hydrographic properties and the resulting flow fields have been employed for the study of the seasonal characteristics of the North Aegean circulation. We performed a long-term simulation with a fine resolution model, which was forced with climatological heat, salt and momentum fluxes at the surface and received input from coarser simulations at the south boundary, where a one-way nesting procedure was applied. The initial conditions were based on a long-term climatological simulation of the coarser intermediate and basin-wide models. This technique provided a strong connection of the limited area model simulation with the Mediterranean basin at large. The regional ALERMO model provided hydrographic fields that have reached a satisfactory climatological cycle and include basic features of the circulation, as is known from previous studies (see Korres and Lascaratos, 2003).

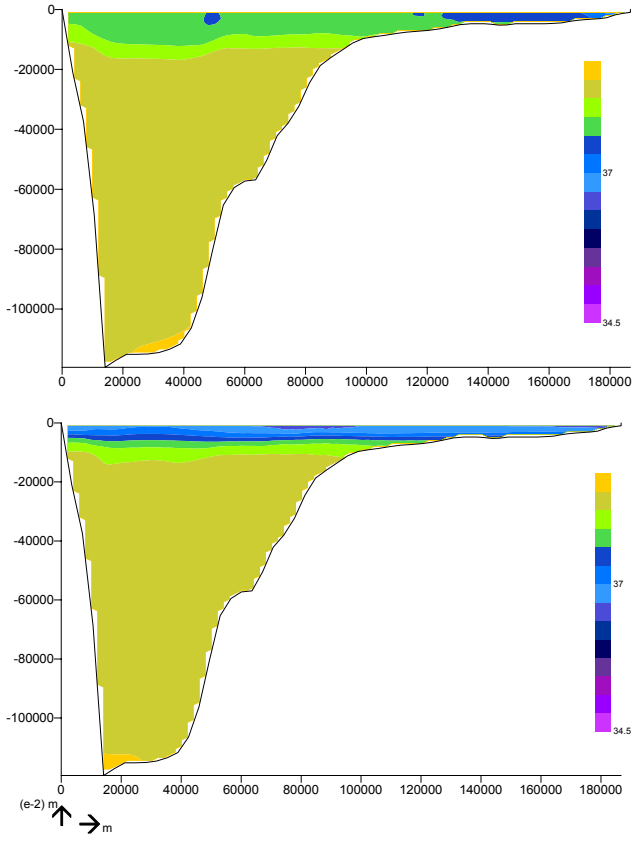

Fig. 13. Salinity cross-section 4 (transect shown on Fig. 1). Winter (upper panel) and Autumn (lower panel).

The North Aegean Model is calculated fields have retained great similarity with the ALERMO distributions of physical properties, while introducing additional features. The fine grid results were 10-day averaged and compared with the corresponding 10-day averages of the ALERMO results at several depths. An example is shown in Fig. 15, where the near-surface salinity for the month of August is shown, as computed from parallel runs of the fine resolution North Aegean Model and the coarser resolution ALERMO model (third year of integration for both models). There is a strik-

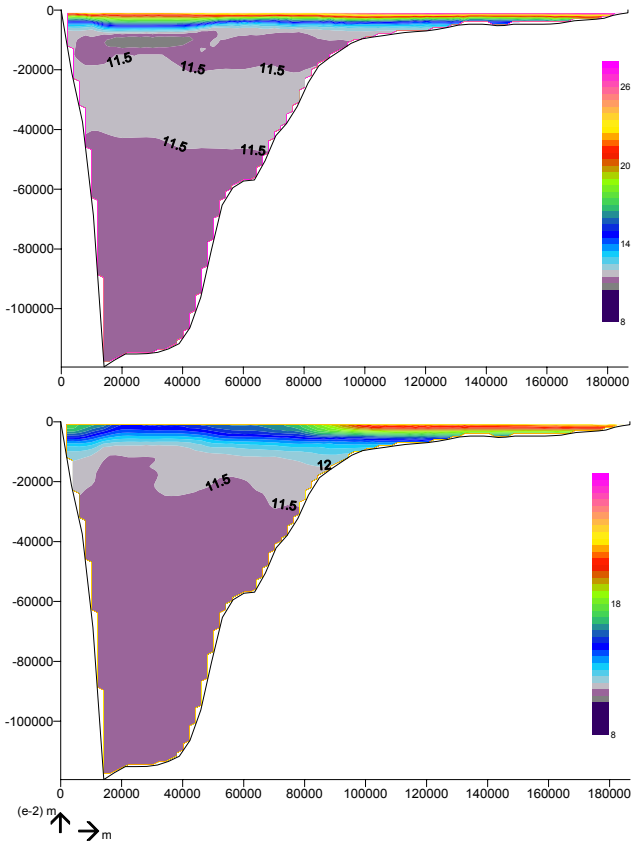

Fig. 14. Temperature cross-section 4 (transect shown on Fig. 1). Summer (upper panel) and Autumn (lower panel).

ing resemblance between the two results, especially in the southern part of the fine grid domain and everywhere but the shallow parts of the northern areas. Throughout the simulations, the similarities were satisfactory in the major circulation features, offering a qualitative validation of fine grid model results and of the coupling method. There were noticeable differences between the two models, which we attribute to certain characteristics of the North Aegean Model: high resolution (about double of that in the ALERMO) that allows not only for a more energetic eddy field, but also for the resolution of narrow passages that guide the flow, detailed coastal topography that starts from 10 m depth (versus 50 m minimum depth in ALERMO), and the seasonal variability in the volume and properties of the BSW outflow (as opposed to the constant annual average of 10 000 m^3s^{-1} used in the ALERMO).

The North Aegean Model results showed intense seasonal variability, with strong flow patterns and substantial horizontal and vertical gradients. We attribute this variability to a) the outflow of waters of Black Sea origin, which have lower salinity (but generally different temperature, too) than the North Aegean waters; b) the preferential heating/cooling between the shelf and deep areas of the domain; c) the intrusion of south Aegean waters; d) the intense topography and e) the dominant northerly component of the imposed wind stress.

The fresh water balance for the Northern Aegean includes the rates of evaporation E, precipitation P, river run-off R and the flow of waters of Black Sea origin BSW, and can be expressed as: $E-(P+R+f_wBSW)$, where f_w is a freshwater factor that represents the amount of BSW that is equivalent to a river-like fresh water flow. The domain area is $6.7{\cdot}10^{10}$m^2. Based on Tables 1 and 2, R=80 mm yr^{-1} and BSW=4500 mm yr^{-1}. From Table 3, P=790 mm yr^{-1} and E=1460 mm yr^{-1}, as calculated from the latent heat flux divided by the latent heat of vaporization $L_E = 2.5008{\cdot}10^6 Jkg^1$ and the density of seawater ρ=1023 kg m^{-3}. Also from Table 3, an annual average for the BSW temperature and salinity is estimated as 16°C and 25 psu, respectively; this yields a density of σ_t =18.2, expressed in "σ-units". The annually averaged properties of temperature and salinity for the upper part of the water column in the North Aegean Model were calculated as 18°C and 37 psu, respectively, or σ_t' =26.5. We express the freshwater conversion factor as: $f_w = (\sigma_t' - \sigma_t)/\sigma_t'$, so that for freshwater input (as for rivers) $f_w \approx 1$, while f_w decreases as the density of the incoming water increases and becomes zero for incoming water of the same density. Then, for BSW f_w is about 0.3, or approximately 30% of the BSW outflow in the Aegean is equivalent to a riverine input.

The above values yield a negative fresh water balance of

$$[E-(P+R+f_wBSW)]_{\text{NorthAegean}} =$$

$$1460-(790+80+1350)\,\text{mm yr}^{-1}$$

or about -0.8 m yr^{-1}, characterizing the Northern Aegean as a "dilution" basin. The excess of fresh water is balanced by the inflow of higher salinity waters from the Eastern Levantine Sea that enter the study domain through the Southern Aegean. It should be noted that all major fresh water lateral inputs for the entire Aegean Sea are introduced in the Northern Aegean. The fresh water budget calculation shows that the Northern Aegean Sea can be considered a dilution basin, largely due to the large flux of fresh water associated with the input at the Dardanelles Strait. Indeed, a "classical" fresh water balance of $E-(P+R)$ would have yielded a salt gain, which is common for the Mediterranean at large. The importance of lateral fresh water inputs in regional Mediterranean seas has been shown in other studies, as for the Adriatic Sea, where the flux due to rivers changes the fresh water balance from positive to negative; Zavatarelli et al. (2002) estimated a gain in fresh water ranging from 0.85 to 1 m yr^{-1}.

The BSW outflow forms a strong plume that occupies the upper part of the water column in the small "Dardanelles channel" and the Aegean basin in the vicinity of the Straits. A return flow exists at the lower layers, forming a crude representation of an estuarine type of circulation within the channel (outflow at the surface, inflow at larger depths). Near the outflow mouth, the anticyclonic bulge forms, as is typical for a river-type plume. The strength of this anticyclone is directly associated with the rate and density of the discharge, as the imposed (climatological) wind field is too low to affect the area of strongest buoyancy forcing and it also

Table 3. Monthly Evolution of Air-sea Fluxes in Limnos Basin

Time (Months)	Wind stress 10^{-2} Nt m^{-2}	Downward Solar Radiation W m^{-2}	Net Upward Flux W m^{-2}	Latent Heat Flux W m^{-2}	Precipitation mm
January	3.9	61.2	274.0	119.0	133.0
February	5.2	89.3	267.0	117.0	80.9
March	3.8	144.0	219.0	92.6	76.7
April	1.1	218.0	143.0	49.9	49.3
May	1.4	283.0	133.0	45.6	49.3
June	1.2	344.0	116.0	35.5	66.8
July	2.5	353.0	145.0	61.6	35.0
August	3.1	305.0	160.0	75.8	31.4
September	3.0	229.0	198.0	95.3	34.7
October	4.6	142.0	250.0	122.0	62.0
November	3.2	78.9	271.0	126.0	85.9
December	3.0	58.0	275.0	120.0	103.0

lacks temporal and spatial variability. As seen in Table 1, the outflow is strongest in late spring to early autumn, peaking in summer. These are also the periods of lowest density for the outflow. The consequences were evident on the surface salinity plots, where the strongest anticyclonic plume bulge was found in summer. This is the only season where there is a tendency to form a northward coastal current, i.e. the buoyancy-driven flow regime that characterises a river-type plume. This northward current is evident in Fig. 5, but rather than hugging the coast toward northeast, it is deflected westward by the northeasterly winds and then branches around the island of Samothraki. However, part of this current enters the Melas Gulf (Fig. 1), where it makes a cyclonic turn to join the branch north of Samothraki. Another interesting feature associated with the strong summer plume is to the south of the Dardanelles, where part of the low-salinity waters is channeled southward between Asia Minor and the Tenedos Island, but then is deflected first back toward the main bulge due to Coriolis (Kourafalou et al., 1996) and then westward, due to the northeasterly wind. During autumn, the Dardanelles plume is still quite strong, forming an anticyclonic bulge near the channel mouth, that is not as pronounced as in summer and is confined between Asia Minor and the Imvros Island. In winter and spring the bulge is even weaker, allowing the wind to deflect it westward, between Imvros and Limnos, with branching around the islands.

We conclude that the conditions that influence the Dardanelles plume are of primary importance for the transport of BSW in the northern Aegean and, consequently, for the southern Aegean and the Eastern Mediterranean at large. The topography in the vicinity of the Dardanelles is also important, as it guides the flow between narrow passages. We have used a careful parameterisation of the Dardanelles outflow, seeking to elaborate on the importance of the differences in discharge rates and physical properties of the outflow for the different seasons. We feel that this has been valuable for the purposes of the present study. Our results suggest that realistic simulations in the North Aegean have to include high frequency buoyancy forcing at the Dardanelles, a very difficult task given the lack of related data. An intermediate step would be to use the discharge rates and vertical structure of the outflow proposed by Besiktepe et al. (1993), as in the numerical simulations of the Aegean by Krestenitis and Valioulis (1997).

Our findings point out that the dominant pathways for BSW are related to the near field distribution described above and to the upper level transport associated with the wind. Here, we have to include the effect of stratification due to heat flux. When the water column is fairly well-mixed, as in winter and spring, offshore transport of BSW waters is weak. During the stratified seasons (summer and autumn), the northerly winds act on a thin upper layer, so that westward transport is intensified. At the same time, the amount of available BSW is larger, so that the effect is more pronounced. Thus, we have a clear indication of BSW reaching the western part of the basin, with a tendency to intrude in northern coastal areas, as far as Thermaikos Gulf. This agrees with satellite pictures and in situ measurements, as was shown in Zodiatis and Balopoulos (1993) and Zodiatis (1994), while BSW waters were found to enter Thermaikos in autumn (data presented in Kontoyiannis et al., 2003).

The near-surface waters in the north and central parts of the northern Aegean are clearly dominated by a thin layer of low-salinity and occasionally low-temperature waters associated with BSW. This agrees with the observational evidence discussed in Zervakis et al. (2000). They suggest that this condition interferes with dense water formation in the North Aegean, a process that has basin-wide implications for the Mediterranean. They point out that the Skyros basin, which is away from substantial BSW influence, exhibits higher salinity than the deep basins in the North Aegean trough. This is reproduced in the model simulation, as a comparison of salinity in the deep parts of the Skyros basin (Fig. 9) and the Sporades basin (Fig. 13) reveals. The potential of dense water formation in the northern part of the domain (supported by observations in Theoharis and Geor-

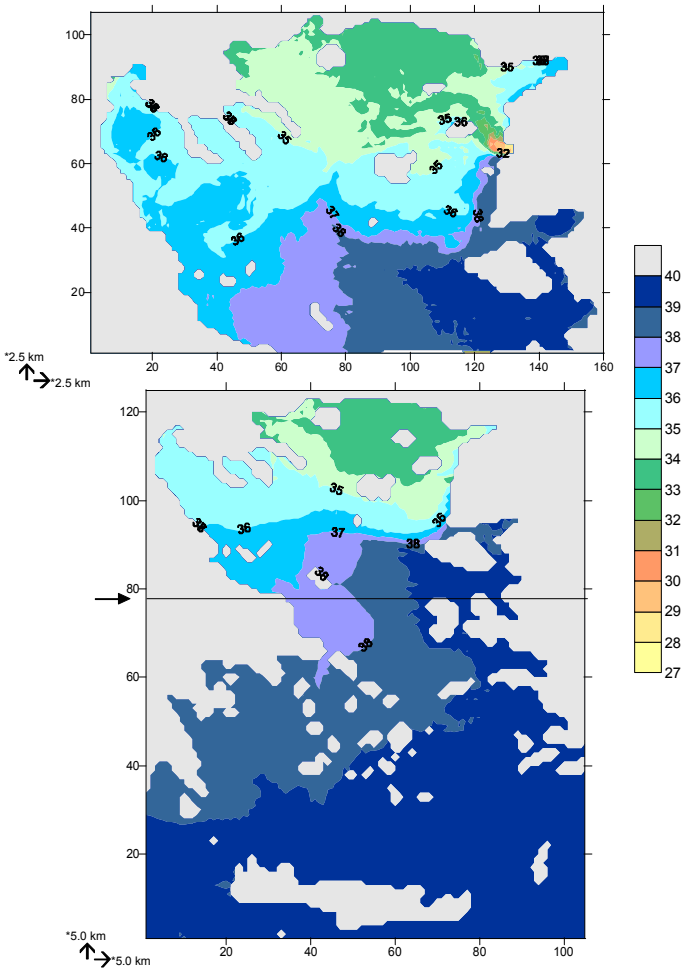

Fig. 15. Model computed salinity at 2 m for the month of August (salinity increment: 1 psu); results from the high resolution Aegean shelf model (upper panel) and the coarser regional ALERMO model (lower panel). The line marked by arrow shows the nesting interface between the two models.

gopoulos, 1993) was indicated in the discussion of the vertical structures. For instance, cold surface waters, formed on the north shelf areas (Figs. 8 and 10) in winter, descended in the spring and summer at intermediate levels, insulated from the surface by warmer upper waters, while by autumn they had decreased the temperature of the deep layers, as shown in Fig. 2 for the Athos basin.

The fine resolution of the model allowed the development of a rich eddy field. Certain features, such as the Sporades and Athos anticyclones are semi-permanent and well known from observations (Durrieu de Madron et al., 1992; Zervakis et al., 2000; Kontoyiannis et al., 2003), while they are shown in coarse model results with climatological type forcing (Valioulis and Krestenitis, 1994; Korres and Lascaratos, 2003). The latter suggests that these features are largely controlled by topography and the northerly component of the wind stress. A robust feature at all seasons and at both surface and intermediate depths was the cyclone in the north Skyros basin. An eddy over the depression south of the island of Lesvos appeared generally anticyclonic at intermediate levels, depending on the path of the LIW intrusion, while it exhibited a weaker near surface signal that was found to be cyclonic in winter and anticyclonic in spring.

The numerical results establish the interaction between shelf and deep areas in the North Aegean. This takes the form of intrusions of waters with different properties, especially near surface, where the strong northward and westward advection of modified BSW during the seasons of high vertical stratification (summer and autumn) clearly affects the hydrography of the gulfs around the Chalkidiki peninsula. It also takes the form of a feedback from the shelf areas to the deep sea, through the transport of dense waters that are formed on the shallow parts during the cold winter months that slowly descend toward the deep basins. This is a process that has the potential for long-term effects, as was shown by Zervakis et al. (2000), based on several years of data. They argued that the dense waters that originated from the north Aegean shelf areas can generally remain in the adjacent deep basins for long periods, due to the difficulty in flowing over separating sills that exceed the thickness of the bottom layers.

However, they document two cases of strong cooling events (1987 and 1993) that produced massive quantities of dense waters, so that, together with the old dense waters that were trapped in the troughs, they could overflow the sills and exit toward the southern Aegean with consequences to the larger scale basin circulation.

The results presented here were employed to elucidate the major processes that influence the seasonal variability in the circulation of the North Aegean Sea: inflow of waters of Black Sea origin, wind stress, atmospheric heat and salt fluxes and interaction with the South Aegean. In order to study the interannual variability, temporally and spatially varying values for the related parameters must be employed. This will also allow for the study of flow events related to the episodic nature of the main circulation forcing mechanisms for this area. This is a future plan, as an important step toward the building of a Northern Aegean Sea model with operational predictive capabilities.

Acknowledgements. The study was funded by the EU 5th Framework Programme for the MFSPP Project (Mediterranean Forecast System Pilot Project, MAS3-CT98-0171). K. Barbopoulos was partially supported as a Ph.D. candidate at the Aristotle University of Thessaloniki. A. Karageorgis kindly provided the basic map used in Fig. 1. The authors greatly benefited from discussions on modeling issues with partners in MFSPP. Two anonymous reviewers gave useful remarks that improved the manuscript.

Topical Editor N. Pinardi thanks two referees for their help in evaluating this paper.

References

Besiktepe, S., Ozsoy, E. and Unluata, U.: Filling of the Marmara Sea by the Dardanelles lower layer inflow, Deep-Sea Res. I, 40, 9, 1815–1838, 1993.

Bignami, F., Marullo, S., Santoleri, R., and Schiano, M.: Longwave radiation budget in the Mediterranean Sea, J. Geophys. Res., 100(C2), 2501–2514, 1995.

Blumberg, A. F. and Mellor, G. L.: Diagnostic and prognostic numerical circulation studies of the South Atlantic Bight, J. Geophys. Res., 88(C8), 4579–4592, 1983.

Brasseur, P., Beckers, J. M., Brankart, J. M., and Schoenauen, R.: Seasonal temperature and salinity fields in the Mediterranean Sea: climatological analyses of a historical data set, Deep-Sea Res., 43, 159–192, 1996.

Durrieu de Madron, X., Nyffeler, F., Balopoulos, E. T., and Chronis, G.: Circulation and distribution of suspended matter in the Sporades Basin (northwestern Aegean Sea), J. Mar. Syst., 3, 237–248, 1992.

Jaeger, L.: Monatskarten des Niederschlags für die ganze Erde, Berichte des Deutschen Wetterdienstes, in German, 18(139), 1–38, 1976.

Kondo, J.: Air-sea bulk transfer coefficients in diabatic conditions, Boundary-Layer Meteorology, 9, 91–102, 1975.

Kontoyiannis, H., Kourafalou, V. H., and Papadopoulos, V.: The seasonal characteristics of the hydrology and circulation in the Northwest Aegean Sea (Eastern Mediterranean): observations and modeling, J. Geophys. Res., accepted, 2003.

Kourafalou, V. H., Oey, L.-Y., Wang, J. D., and Lee, T. N.: The fate of river discharge on the continental shelf. Part I: modelling the river plume and the inner-shelf coastal current, J. Geophys. Res., 101(C2), 3415–3434, 1996.

Kourafalou, V. H.: Process studies on the Po River plume, North Adriatic Sea, J. Geophys. Res., 104(C2), 29 963–29 985, 1999.

Kourafalou, V. H., Savvidis, Y. G., Krestenitis, Y. N., Koutitas, C. G., and Barbopoulos, K. A.: Modelling studies on the processes that influence matter transfer on the Gulf of Thermaikos (North Aegean Sea), submitted to Continental Shelf Research, 2003.

Korres, G. and Lascaratos, A.: A one-way nested, eddy resolving model of the Aegean and Levantine basins: Implementation and climatological runs, Ann. Geophysicae, this issue, 2003.

Krestenitis, Y. N. and Valioulis, I. A.: The Black Sea Waters influence to the seasonal baroclinic circulation of the Aegean Sea, Proceedings of the Third International Conference on the Mediterranean Coastal Environment, (Ed) Özhan, E., MEDCOAST 97, 11–14 November, Qawra, Malta, 1997.

Mellor, G. L. and Yamada, T.: Development of a turbulence closure model for geophysical fluid problems, Rev. Geophys. Space Phys., 20(4), 851–875, 1982.

Pinardi, N., Allen, I., Demirov, E., De Mey, P., Korres, G., Lascaratos, A., Le Traon, P.-Y., Maillard, C., Manzella, G., and Tziavos, C.: The Mediterranean ocean Forecasting System: first phase of implementation (1998–2001), Ann. Geophysicae, this issue, 2003.

Poulos, S. E., Drakopoulos, P. G., and Collins, M. B.: Seasonal variability in sea surface oceanographic conditions in the Aegean Sea (Eastern Mediterranean): an overview, J. Mar. Systems, 225–244, 1997.

Reed, R. K.: On estimating insolation over the ocean, J. Phys. Oceanogr., 17, 854–871, 1977.

Smagorinsky, J.: General circulation experiments with the primitive equations, I. The basic experiment, Mon. Weather Rev., 91, 99–164, 1963.

Theoharis, A. and Georgopoulos, D.: Dense water formation over the Samothraki and Limnos plateaux in the North Aegean Sea (Eastern Mediterranean Sea), Cont. Shelf Res., 13(8/9), 919–939, 1993.

Therianos, A. D.: Rainfall and geographical distribution of river runoff in Greece, Bull. Geol. Soc. Greece, XI, 28–58, in Greek, 1974.

Valioulis, I. and Krestenitis, Y.: Modelling the Water Mass Circulation in the Aegean Sea. Part I. Wind Stresses, Thermal and Haline Fluxes, Ann. Geophysicae, 12, 794–807, 1994.

Ünlüata, Ü., Oguz, T., Latif, M. A., and Özsoy, E.: On the physical oceanography of the Turkish Straits. In: The physical oceanography of sea straits, (Ed) Pratt, J., NATO-ASI series, Kluwer Academic, The Netherlands, pp. 25–60, 1990.

Zavatarelli, M., Pinardi, N., Kourafalou, V. H., and Maggiore, A.: Diagnostic and prognostic model studies of the Adriatic Sea general circulation. Part 1: The seasonal variability and the role of the forcing functions, J. Geophys.Res., 107(C1), 4/1–4/20, 2002.

Zervakis, V., Georgopoulos, D., and Drakopoulos, P. G.: The role of the North Aegean in triggering the recent Eastern Mediterranean climatic changes, J. Geophys. Res., 105(C11), 26 103–26 116, 2000.

Zodiatis, G.: Advection of the Black Sea water in the north Aegean Sea, Global Atmos. Ocean Syst., 2(1), 41–60, 1994.

Zodiatis, G. and Balopoulos, E.: Structure and characteristics of fronts in the North Aegean Sea, Bolletino in Oceanologica Theorica ed Applicata, XI(2), 113–124, 1993.